Deep-sequencing reveals broad subtype-specific HCV resistance mutations associated with treatment failure

Qian Chen[a,b,1], Celia Perales[a,b,1], María Eugenia Soria[a], Damir García-Cehic[a,b], Josep Gregori[a,b,c], Francisco Rodríguez-Frías[b,d], María Buti[a,b], Javier Crespo[e], José Luis Calleja[f], David Tabernero[b,d], Marta Vila[d], Fernando Lázaro[g], Ariadna Rando-Segura[d], Leonardo Nieto-Aponte[d], Meritxell Llorens-Revull[a,b], Maria Francesca Cortese[d], Irati Fernandez-Alonso[a], José Castellote[h], Jordi Niubó[i], Arkaitz Imaz[j], Xavier Xiol[h], Lluís Castells[a,b], Mar Riveiro-Barciela[a,b], Jordi Llaneras[a,b], Jordi Navarro[k], Víctor Vargas-Blasco[a,b], Salvador Augustin[a,b], Isabel Conde[b,l], Ángel Rubín[b,l], Martín Prieto[b,l], Xavier Torras[b,m], Nuria Margall[n], Xavier Forns[b,o], Zoe Mariño[b,o], Sabela Lens[b,o], Martin Bonacci[o], Sofía Pérez-del-Pulgar[b,o], Maria Carlota Londoño[b,o], María Luisa García-Buey[p], Paloma Sanz-Cameno[p], Rosa Morillas[q], Elisa Martró[r], Verónica Saludes[r], Helena Masnou-Ridaura[q], Javier Salmerón[b,s], Rosa Quíles[b,s], José Antonio Carrión[b,t], Montserrat Forné[u], Mercè Rosinach[u], Inmaculada Fernández[v], Javier García-Samaniego[b,w], Antonio Madejón[b,w], Pilar Castillo-Grau[w], Carme López-Núñez[x], María José Ferri[y], Rosa Durández[z], Federico Sáez-Royuelaa[a,2], Moisés Diagoa[b], Concepción Gimeno[ac], Rafael Medina[ac], Juan Buenestado[ad], Albert Bernet[ae], Juan Turnes[af], Matilde Trigo-Daporta[ag], Manuel Hernández-Guerra[ah], Manuel Delgado-Blanco[ai], Angelina Cañizares[aj], Juan Ignacio Arenas[ak], Maria Juana Gomez-Alonso[f], Manuel Rodríguez[al], Elisabet Deig[am], Gemma Olivé[an], Oscar del Río[an], Joaquín Cabezas[e], Ildefonso Quiñones[ao], Mercè Roget[ap], Silvia Montoliu[aq], Juan García-Costa[ar], Lluís Force[as], Silvia Blanch[at], Miguel Miralbés[au], María José López-de-Goicoechea[av], Angels García-Flores[aw], María Saumoy[j], Teresa Casanovas[h], Carme Baliellas[h], Pau Gilabert[h], Albert Martin-Cardona[h], Rosa Roca[h], Mercè Barenys[ax], Joana Villaverde[h], Silvia Salord[h], Blau Camps[h], María Silvan di Yacovo[h], Imma Ocaña[k], Silvia Sauleda[a,b,ay], Marta Bes[a,b,ay], Judit Carbonell[a], Elena Vargas-Accarino[a], Sofía P. Ruzo[a], Mercedes Guerrero-Murillo[a], Georg Von Massow[a], María Isabel Costafreda[a,ay], Rosa Maria López[d], Leticia González-Moreno[p], Yolanda Real[p], Doroteo Acero-Fernández[x], Silvia Viroles[x], Xavier Pamplona[x], Mireia Cairó[u], María Dolores Ocete[ac], José Francisco Macías-Sánchez[an], Angel Estébanez[e], Joan Carles Quer[aq], Álvaro Mena-de-Cea[ai], Alejandra Otero[ai], Ángeles Castro-Iglesias[ai], Francisco Suárez[ai], Ángeles Vázquez[ai], David Vieito[ai], Soledad López-Calvo[ai], Pilar Vázquez-Rodríguez[ai], Francisco José Martínez-Cerezo[ar], Raúl Rodríguez[ar], Ramiro Macenlle[ar], Alba Cachero[ba], Gasshan Mereish[ba], Carme Mora-Moruny[bb], Silvia Fábregas[bb], Begoña Sacristán[bc], Agustín Albillos[bd], Juan José Sánchez-Ruano[be], Raquel Baluja-Pino[bf], Javier Fernández-Fernández[bf], Carlos González-Portela[bf], Carmen García-Martin[bg], Gloria Sánchez-Antolín[bh], Raúl Jesús Andrade[bi], Miguel Angel Simón[bj], Juan Manuel Pascasio[bk], Manolo Romero-Gómez[b,bl], José Antonio del-Campo[b,bl], Esteban Domingo[b,bm], Rafael Esteban[a,b], Juan Ignacio Esteban[a,b], Josep Quer[a,b].

[a] Liver Unit, Liver Diseases - Viral Hepatitis, Vall d'Hebron Institut of Research (VHIR), Hospital Universitari Vall d'Hebron (HUVH), Barcelona, Spain

[b] Centro de Investigación Biomédica en Red de Enfermedades Hepáticas y Digestivas (CIBERehd), Instituto de Salud Carlos III, Madrid, Spain

[c] Roche Diagnostics SL, Sant Cugat del Valles, Barcelona, Spain

[d] Biochemistry and Microbiology Department, VHIR-HUVH, Barcelona, Spain

[e] Gastroenterology and Hepatology Department, Instituto de Investigación (IDIVAL), Hospital Universitario Marqués de Valdecilla, Santander, Spain

[f] Liver Unit, Hospital Universitario Puerta de Hierro, Madrid, Spain

[g] Microbiology Department, Hospital Universitario La Paz, Madrid, Spain

[h] Liver Unit, Hospital Universitari de Bellvitge, Barcelona, Spain

[I] Microbiology Department, Hospital Universitari de Bellvitge, Barcelona

[j] HIV and STI Unit, Infectious Diseases Department, Hospital Universitari de Bellvitge, Barcelona, Spain

[k] Infectious Disease Unit, HUVH, Barcelona, Spain

[l] Liver Unit, Hospital Universitario La Fe, Valencia, Spain

[m] Microbiology Department, Hospital Universitari Santa Creu i Sant Pau, Barcelona, Spain

[n] Digestive Pathology Unit, Hospital Universitari Santa Creu i Sant Pau, Barcelona, Spain

[o] Liver Unit, Institut d'Investigacions Biomèdiques August Pi i Sunyer (IDIBAPS) - Hospital Clínic de Barcelona, Barcelona, Spain

[p] Liver Unit, Hospital Universitario La Princesa, Madrid, Spain

[q] Liver Unit, Hospital Universitari Germans Trias i Pujol, Barcelona, Spain

[r] Microbiology Department, Centro de Investigación Biomédica en Red de Epidemiología y Salud Pública (CIBERESP), Institut de Recerca Germans Trias i Pujol (IGTP), Hospital Universitari Germans Trias i Pujol, Barcelona, Spain

[s] Liver Unit, Complejo Hospitalario de Granada, Granada, Spain

[t] Liver Unit, Parc de Salut Mar - Hospital del Mar, Barcelona, Spain

[u] Gastroenterology Unit, Hospital Universitari Mútua Terrassa, Spain

[v] Liver Unit, Hospital Universitario 12 de Octubre, Madrid, Spain

[w] Liver Unit, Instituto de Investigación Hospital Universitario La Paz (IdiPAZ) - Hospital Universitario La Paz, Madrid, Spain

[x] Gastroenterology Department, Hospital Universitari Doctor Josep Trueta, Girona, Spain

[y] Clinical Laboratory, Hospital Universitari Doctor Josep Trueta, Girona, Spain

[z] Laboratori Territorial - Hospital Santa Caterina, Girona, Spain

[aa] Gastroenterology and Hepatology Depart., Hospital Universitario de Burgos, Burgos, Spain

[ab] Liver Unit, Hospital General de Valencia, Valencia, Spain

[ac] Microbiology Unit, Hospital General de Valencia, Valencia, Spain

[ad] Medicine Department-Medical School, Hospital Univ. Arnau de Vilanova, Lleida, Spain

[ae] Microbiology Department, Hospital Universitari Arnau de Vilanova, Lleida, Spain

[af] Gastroenterology and Hepatology Department, Instituto de Investigación Sanitaria Galicia Sur (IISGS) - Complejo Hospitalario de Pontevedra, Pontevedra, Spain

[ag] Microbiology and Parasitology Department, Complejo Hospitalario de Pontevedra, Pontevedra, Spain

[ah] Liver Unit, Hospital Universitario de Canarias, La Laguna, Santa Cruz de Tenerife, Spain

[ai] Liver Unit, Complejo Hospitalario Universitario A Coruña (CHUAC), La Coruña, Spain

[aj] Microbiology Department, Institut de Investigación Biomédica de a Coruña (INIBIC) - Complejo Hospitalario Universitario A Coruña (CHUAC), La Coruña, Spain

[ak] Gastroenterology, Hospital Universitario Donostia, San Sebastián, Spain

[al] Gastroenterology Depart., Central University Hospital of Asturias (HUCA), Oviedo, Spain

[am] Granollers General Hospital, Barcelona, Spain

[an] Sant Jaume de Calella County Hospital, Barcelona, Spain

[ao] Gastroenterology Department, Dr Negrin University Hospital of Gran Canaria, Las Palmas de Gran Canaria, Spain

[ap] Liver Unit, Consorci Sanitari de Terrassa - Hospital de Terrassa, Terrassa, Spain

[aq] Gastroenterology Unit, Joan XXIII University Hospital, Tarragona, Spain

[ar] Virology and Molecular Biology Unit, Microbiology Department, Complexo Hospitalario Universitario de Ourense (CHUO), Ourense, Spain

[as] Hospital de Mataró, Barcelona, Spain

[at] Hospital Universitari Sant Pau i Santa Tecla, Tarragona, Spain

[au] Gastroenterology Department, Hospital Universitari Santa Maria de Lleida, Lleida, Spain

[av] Microbiology Unit, Hospital Universitario de Galdakao, Vizcaya, Spain

[aw] County Hospital of Blanes, Girona, Spain

[ax] Liver Unit, Hospital de Viladecans, Barcelona, Spain

[ay] Banc de Sang i Teixits (BST), Barcelona, Spain

[az] Hospital Universitari Sant Joan de Reus, Tarragona, Spain

[ba] Liver Unit, Hospital d'Igualada, Barcelona, Spain

[bb] Fundació Salut Empordà - Hospital de Figueres, Girona, Spain

[bc] Hospital San Pedro-CIBIR, La Rioja, Logroño, Spain

[bd] Hospital Universitario Ramón y Cajal, Madrid, Spain

[be] *Gastroenterology and Hepatology Department, Hospital Univ.de Toledo, Toledo, Spain*
[bf] *Hospital Povisa, Vigo, Spain*
[bg] *Laboratori de Referència de Catalunya, Barcelona, Spain*
[bh] *Hospital Universitario Río Ortega, Valladolid, Spain*
[bi] *Gastroenterology Unit, Hospital Virgen de la Victoria, Málaga, Spain*
[bj] *Liver Unit, Hospital Universitario Miguel Servet, Zaragoza, Spain*
[bk] *Liver Unit, Hospital Universitario Virgen del Rocío, Seville, Spain*
[bl] *Liver Unit, Hospital Universitario Virgen de Valme, Seville, Spain*
[bm] *Centro de Biología Molecular "Severo Ochoa" (CBMSO), Universidad Autónoma de Madrid, Madrid, Spain*

Abstract

A percentage of hepatitis C virus (HCV)-infected patients fail direct acting antiviral (DAA)-based treatment regimens, often because of drug resistance-associated substitutions (RAS). The aim of this study was to characterize the resistance profile of a large cohort of patients failing DAA-based treatments, and investigate the relationship between HCV subtype and failure, as an aid to optimizing management of these patients.

A new, standardized HCV-RAS testing protocol based on deep sequencing was designed and applied to 220 previously subtyped samples from patients failing DAA treatment, collected in 39 Spanish hospitals. The majority had received DAA-based interferon (IFN) α-free regimens; 79% had failed sofosbuvir-containing therapy. Genomic regions encoding the nonstructural protein (NS) 3, NS5A, and NS5B (DAA target regions) were analyzed using subtype-specific primers.

Viral subtype distribution was as follows: genotype (G) 1, 62.7%; G3a, 21.4%; G4d, 12.3%; G2, 1.8%; and mixed infections 1.8%. Overall, 88.6% of patients carried at least 1 RAS, and 19% carried RAS at frequencies below 20% in the mutant spectrum. There were no differences in RAS selection between treatments with and without ribavirin. Regardless of the treatment received, each HCV subtype showed specific types of RAS. Of note, no RAS were detected in the target proteins of 18.6% of patients failing treatment, and 30.4% of patients had RAS in proteins that were not targets of the inhibitors they received.

HCV patients failing DAA therapy showed a high diversity of RAS. Ribavirin use did not influence the type or number of RAS at failure. The subtype-specific pattern of RAS emergence underscores the importance of accurate HCV subtyping. The frequency of "extra-target" RAS suggests the need for RAS screening in all three DAA target regions.

1.Introduction

Hepatitis C virus (HCV) chronic infection is the leading cause of liver-related morbidity and mortality worldwide. In Spain, an estimated 0.5% of the population has active HCV infection (HCV RNA in plasma), and 1.1% has antibodies against HCV. The United Nations General Assembly has adopted a resolution to combat all 5 viral hepatitis, with particular focus on HBV and HCV (Polaris Observatory HCV Collaborators, 2017; United Nations-General Assembly, 2017). In keeping with this effort, the Spanish National Healthcare System approved the Strategic Plan for Tackling Hepatitis C (PEAHC, Plan Estratégico Nacional Contra la Hepatitis C) in March 2015, "to improve the prevention, diagnosis, treatment, and follow-up of HCV-infected patients" (Ministry of health social services and equality, 2018). According to updated data from the Spanish Ministry of Health, around 130,000 chronic HCV patients have been treated with direct-acting antiviral (DAA)-based regimens within the Plan. Among them, 95.5% have achieved virologic cure, whereas 4.5% have failed DAA treatment and are under consideration for retreatment (Ministry of health social services and equality, 2019).

Treatment failure has been associated with selection of resistance-associated substitutions (RAS) in the viral genome that confer decreased susceptibility to DAAs, generate cross-resistance with other inhibitors of the same class, and render salvage treatments more expensive and difficult (Buti et al., 2015; Dietz et al., 2018; EASL, 2018; Lontok et al., 2015; Sarrazin, 2016; Vermehren and Sarrazin, 2012; Kanda et al., 2017; Sorbo et al., 2018). Retreatment strategies are particularly hampered in cases of multidrug resistance, which challenges the possibility to switch DAA class.

Following treatment failure, RAS in nonstructural protein (NS) 3 often become undetectable within months after stopping therapy, whereas NS5A RAS can persist for years (Sarrazin, 2016). NS5A RAS have a negative impact on retreatment outcome in NS5A inhibitor-experienced patients (Lawitz et al., 2015; Sarrazin et al., 2016) and other RAS emerging in the viral population can also have a deleterious effect. Hence, current guidelines state that resistance testing can be useful to guide retreatment in DAA failures according to the resistance profile observed (EASL, 2018; AASLD, 2017). RAS can be detected in clinical samples using population (Sanger) sequencing or deep sequencing with next-generation techniques.

In a recent study including 626 DAA-experienced European patients, the most important RAS associated with treatment failure were detected in the genotype (G) 1 subtypes, G1a and G1b, and in G2, G3, and G4 (Dietz et al., 2018). In another study, Di Maio et al. investigated 200 non-responding patients with G1a, G1b, G1g, G2c, G3a, and G4 infection, and identified extra-target RAS in 9% of samples. A remarkable 57.1% of non-responders had a misclassified genotype (Di Maio et al., 2017). Although these studies provide valuable information, they were performed using Sanger sequencing, which has a relatively low sensitivity: RAS (observed as mixed peaks) must be present at frequencies of at least 15%–20% in the viral population. This may be a limitation for planning retreatment options, as it has been shown that even RAS present at frequencies of less than 15% can be selected and emerge as majority variants following treatment (Perales et al., 2018).

Previous work has shown that a minimum coverage of 10,000 reads (sequences) per amplicon should be reached to identify minority mutants present as at least 1% of the viral population (Gregori et al., 2013). Next-generation sequencing (NGS) has the capability to determine whether certain RAS are undetectable at this extremely low level, which would be important to confirm when deciding on retreatment regimens. However, NGS-based real-life resistance profile data and exhaustive clinical descriptions of patients who fail treatment are largely lacking (Vermehren et al., 2016).

Acquisition of data on RAS emerging in patients failing first-line therapy was considered an essential component of the PEAHC strategy to understand the virus-related variables associated with treatment failure and optimize HCV management in our setting. Hence, the aim of this study was to characterize the resistance profile of a large cohort of patients failing DAA-based treatments, and investigate the relationship between HCV subtype and failure. To this end, a specific analytical protocol using NGS technology was developed in our laboratory.

2. Material and methods

2.1. Patients

HCV-infected patients (N = 220) who failed a DAA treatment from 39 Spanish hospitals adhering to the PEAHC (Fig. S1) were included in the study. The mean sampling time from end of treatment (EOT) was 28 weeks (data available for 128 samples). Serum samples were coded, and all clinical and viral data were recorded in an anonymous database. As samples were analyzed for diagnostic purposes, further patient consent was not required, and a resistance profile report for each sample was sent to physicians. The cohort distribution according to HCV subtype and treatment received is reported in Table 1 and the patients' clinical data in Table S1.

Table 1. Patient distribution according to subtype, DAA regimen, and ribavirin use. (a) G1l; (b) G2i; (c) G2j; (d) G2c; (e) Mixed infection (Mi) 4d (69.3%) + 1b (30.6%); (f) Mi 4a (98.5%) + 1b (1.5%); (g) Mi 1b (80%) + 1a (19.9%); (h) Mi 4d (96.7%) + 3a (3.3%).

| | | Subtypes | | | | | | |
		G1b	G1a	G3a	G4d	Others	Mix	
SOF-based treatments	LDV + SOF (+RBV/-RBV)	12/23	7/21	4/5	10/3	1[a]/0	1[e]/1[f]	35/53
	SMV + SOF (+RBV/-RBV)	18/10	4/2	–	3/1	–	1[g]/0	26/13
	DCV + SOF (+RBV/-RBV)	2/4	0/2	11/16	–	–	–	13/22
	SOF + RBV	3	–	3	–	2[b]	–	8
	SOF + IFN + RBV	–	–	2	–	1[c]	–	3
	GZR + EBR + SOF	–	–	1	–	–	–	1
Non SOF-based treatments	PTV/r + OMV + DSV (+RBV/-RBV)	4/3	6/4	1/2	–	–	–	11/9
	PTV/r + OMV (+RBV/-RBV)	–	1/1	2/0	8/0	–	1[h]/0	12/1
	SMV + DCV (+RBV/-RBV)	0/2	1/0	–	0/1	–	–	1/3
	DCV + IFN + RBV	2	–	–	–	–	–	2
	SMV + IFN + RBV	–	1	–	–	–	–	1
	GZR + EBR + RBV	–	–	–	1	–	–	1
	FDV + DLV (+RBV/-RBV)	2/1	–	–	–	–	–	2/1
	UPF	–	–	–	–	1[d]	–	1
	GLE + PIB	1	–	–	–	–	–	1
	TOTAL (+RBV/-RBV)	43/44	20/30	23/24	22/5	4/1	3/1	220

2.2. Methods

A high-resolution HCV subtyping method (Quer et al., 2015) was used on all samples to accurately identify HCV subtypes and mixed infections, so that subtype-specific primers could be selected to amplify the three DAA-targeted genomic regions of HCV (NS3, NS5A, and NS5B) (Perales et al., 2018).

Amplified products were analyzed using the 454/GS-Junior platform (Quer et al., 2015) up to December 2016, when the platform was discontinued. The method was then adapted to the MiSeq system (Illumina). Comparison of the two platforms (Soria et al., 2018) has shown equivalent performance, with higher resolution power for MiSeq (Table S2) (Perales et al., 2018).

Raw data were analyzed using in-house R scripts, as previously described (Perales et al., 2018), and were compiled in the QSutils program (QSutils, 2018). Briefly, in the first step, reads containing >5% of base pairs with Phred scores below Q30 were discarded. Next, demultiplexing was done to identify reads by specific primer, and clean reads were collapsed into haplotypes. Haplotypes were aligned with the reference sequence for each subtype, and those with more than 2 indeterminations, 3 gaps, or 99 differences were excluded. Reads were translated into amino acids, and the intersection between forward and reverse haplotypes with abundances >0.2% was determined. From these alignments, all variants by site or haplotype present at ≥1% were analyzed; additional details of the method are described elsewhere (Soria et al., 2018). Mean coverage (number of reads sequenced per amplicon) was 31,868 reads for NS3, 36,400 for NS5A, and 40,011 for NS5B.

Because of the considerable intra-subtype diversity of HCV, 1181 sequences were retrieved from the Los Alamos databank to generate a consensus sequence (defined by the most frequent amino acid at each position) for G1a (553 sequences), G1b (427), G1l (3), G2a (7), G2b (79), G2c (8), G2i (4), G2j (8), G2k (4), G2q (2), G3a (49), G3b (4), G3k (2), G4a (18), G4d (5), G4f (6), and G5a (2).

For the present study, extra-target RAS were defined as well-recognized antiviral resistance mutations appearing in NS3, NS5A, or NS5B in patients who were receiving DAAs that targeted regions other than those in which the mutations were found (EASL, 2018; Lontok et al., 2015; Sarrazin, 2016; Sorbo et al., 2018; Donaldson et al., 2015).

3. Results

3.1. Subtype distribution at treatment failure

G1 was the most prevalent (138/220, 62.7%) genotype in the 220 patients, and included subtypes G1a (50/220, 22.7%) and G1b (87/220, 39.5%). These were followed in frequency by G3a in 47/220 (21.4%) and G4d in 27/220 (12.3%). The remaining 3.6% (n = 8/220) belonged to G2j (n = 2), G2c (n = 1), and G2i (n = 1). Four cases of mixed infections were detected (G1b + G1a; G4a + G1b; G4d + G1b; G4d + G3a) (Fig. 1A). Almost half the samples (100/220) had been genotyped using commercial methods before starting treatment at the attending hospitals. In 7 cases, the genotype identified by these methods did not coincide with the genotype obtained using our more accurate high-resolution method (3 G3a were initially assigned to G1, 3 G3a to G4, and 1 G1a to G4).

The HCV subtype distribution closely followed the subtype prevalence in chronically infected patients in the Spanish general population (Rodriguez-Frias et al., 2017) except for G3a, which is found in 8.87% of the population, but was detected in 21.4% of patients who failed treatment. The treatments received are described in Fig. 1B and Table 1.
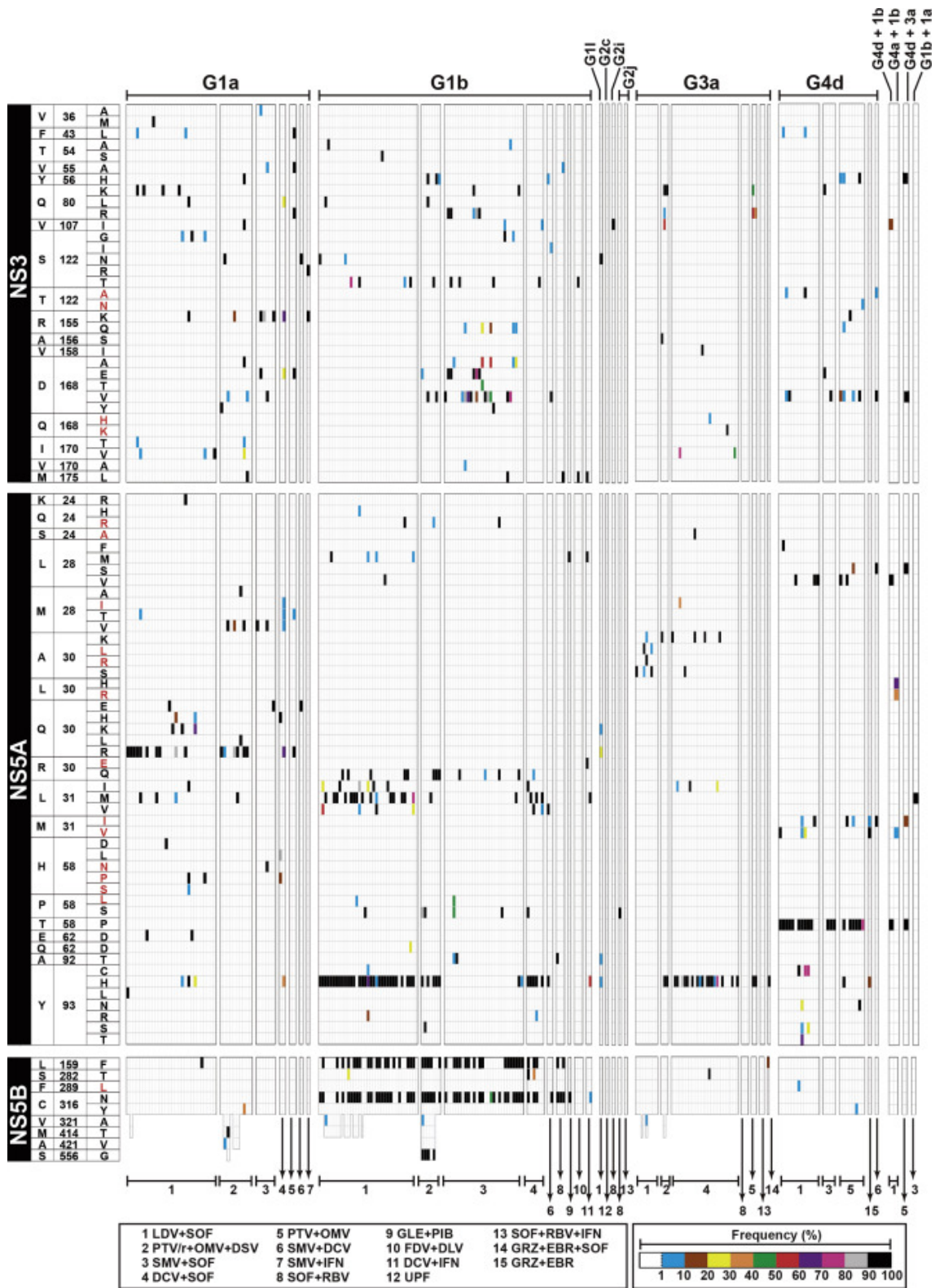
3.2. RAS frequency

Ninety different RAS were identified, 33 mapping in NS3, 48 in NS5A, and 9 in NS5B, corresponding to 551 mutations (Fig. 2). Most RAS (69.5%) were present at frequencies of 90%–100%, whereas 5.8%, 5.6%, and 18.9% were found at 50%–90%, 20%–50%, and 1%–20%, respectively. At least 1 RAS was detected in 195 patients (88.6%). There were no known RAS in samples from 25 patients (11.4%). The average number of RAS per patient (considering all the genomic regions analyzed) was 2.1, 3.4, 1.2, and 2.6 for G1a, G1b, G3a, and G4d, respectively. There were no significant differences in the average number of RAS between patients treated with (n = 115) or without (n = 105) RBV-containing regimens (2.5 vs 2.1, p > 0.317; Mann-Whitney test).

3.3. RAS distribution between subtypes

In general, each HCV subtype showed specific RAS types, regardless of the treatment received. The most prevalent RAS and affected proteins for the major subtypes were the following: Q30R in NS5A for G1a; L31M and Y93H in NS5A, and L159F and C316N in NS5B for G1b; Y93H in NS5A for G3a; and T58P in NS5B for G4d (Fig. 2). Venn diagrams were constructed to determine which RAS were common to the different subtypes. Remarkably, the Q80K substitution in NS3, Y93H in NS5A, and L159F in NS5B (central area of Venn diagram) were the only RAS common to all subtypes (Fig. 3). Of note, Q80K in NS3, found here in G1a, G1b, G3a, and G4d patients, has been previously described only in G1a/1b patients, and L159F has not been previously described in G4d (EASL, 2018; Lontok et al., 2015; Sarrazin, 2016; Donaldson et al., 2015). Some RAS were subtype-exclusive, while others appeared in more than 1 subtype (Fig. 2, Fig. 3).

Fig. 1. HCV subtype distribution in the cohort under study. A) Number of patients per subtype: G1a N = 50, G1b N = 87, G1l N = 1, G2c N = 1, G2i N = 1, G2j N = 2, G3a N = 47, G4d N = 27 and mixed infections G1b + G1a, G4a + G1b, G4d + G1b, and G4d + G3a N = 4 (N = 1 each). B) Percentage of patients who received each DAA treatment type with color darkness indicating inclusion of RBV. The purple slice (11.4%) has been enlarged to report twelve minor treatments (see Table 1 for additional details). Abbreviations: PTV, paritaprevir; r, ritonavir; SMV, simeprevir; GLE, glecaprevir; FDV, faldaprevir; GZR, grazoprevir; DCV, daclatasvir; LDV, ledipasvir; OMV, ombitasvir; EBR, elbasvir; PIB, pibrentasvir; SOF, sofosbuvir; DSV, dasabuvir; DLV, deleobuvir; UPF, uprifosbuvir; RBV, ribavirin.

Fig. 2. Heat map of resistance-associated substitutions (RAS). Each column represents a patient. The target protein (NS3, NS5A or NS5B), the amino acid (one code letter; eg, V), the position in each protein (eg, 36), and the substitution (eg, A or M) are indicated in the 4 columns on the left. The viral subtype (eg, G1a) and mixed infections (eg, G4d + G1b) are indicated at the top. The treatment code (eg, 1, 2 …) is given at the bottom and decoded in a large framed box (eg, 1 LDV + SOF). RAS frequency above the 1% limit of detection is color-coded in each box of the heat map, showing which mutations occurred; the color indicates the frequency at which the mutations were found in the isolate. The frequency code is shown in the bottom right box. Amino acids depicted in red indicate changes previously described as RAS, but with a different wild-type (parental) amino acid than the one indicated. Empty slots mean that no amino acid mutation was observed compared with the subtype reference (wild-type) amino acid sequence.
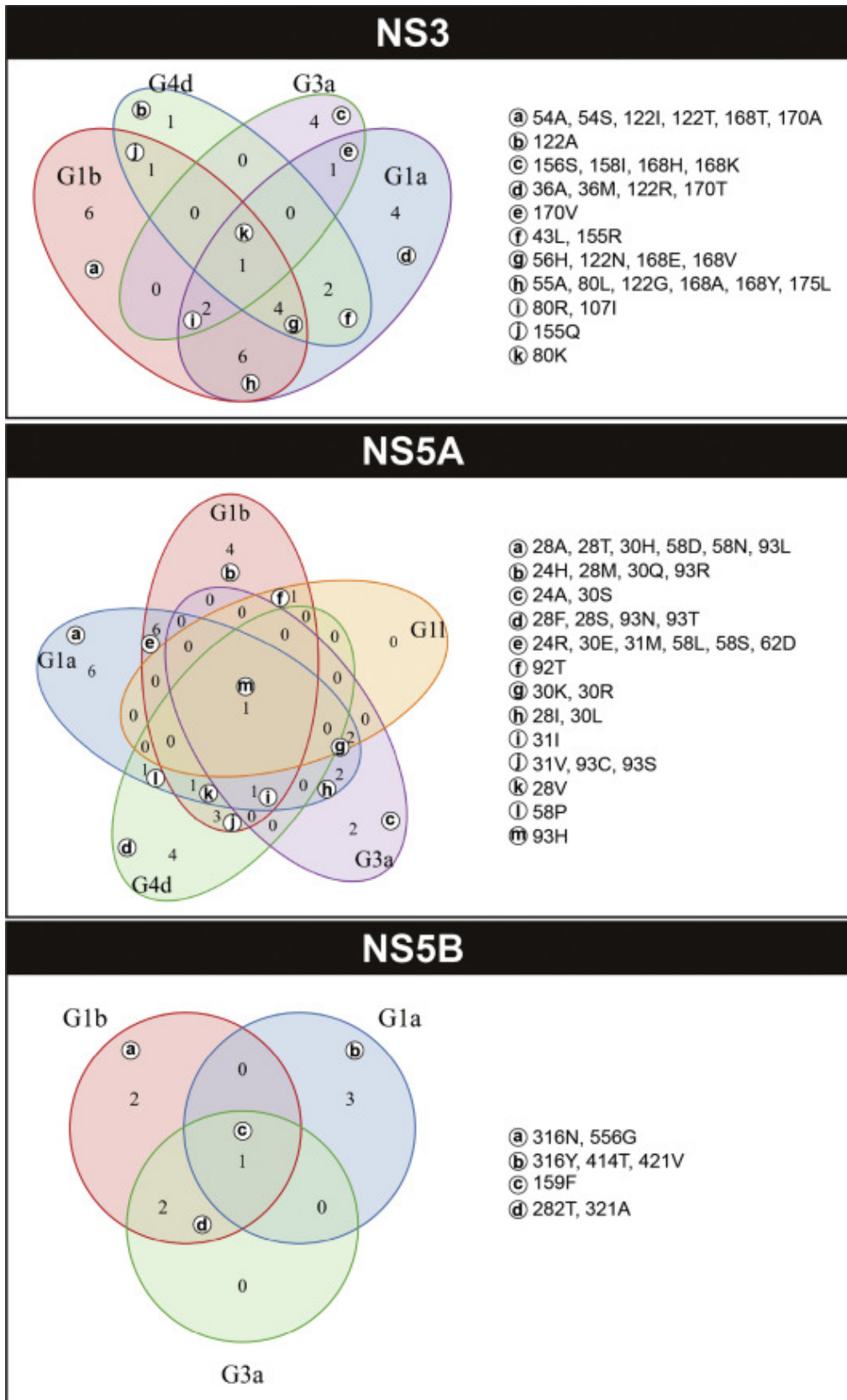
Fig. 3. Venn diagrams represent the number and substitutions shared between the major subtypes according to the target protein. Only subtypes showing more than 1 RAS following treatment failure and RAS present in more than 1 patient are included. Only the mutant amino acid detected at the time of the analyses was included in this analysis, regardless of the wild-type amino acid. The background color in the ellipses identifies the HCV subtype. The numbers indicate the RAS detected in that subtype, whereas numbers in overlapping ellipses denote RAS shared by the different subtypes. Encircled letters define the amino acid substitutions, listed on the right.

3.4. Prevalent RAS associated with the major treatments

3.4.1. Ledipasvir [LDV] + Sofosbuvir [SOF] (n = 88)

The most prevalent RAS in the NS5A region were Q30 R/K/H/E for G1a, L31M/I/V and Y93H for G1b, A30 S/L/R/K for G3a (mutation not previously described in G3a) (Sorbo et al., 2018), and T58P and L28V for G4d. These last 2 substitutions never appeared together, whereas in G1b, L31I/V was always found together with Y93H.

In the NS5B region, L159F and C316N were seen mainly in G1b (minimum p value = 0.001162). The rare S282T variant, which confers strong resistance to SOF in vitro, was detected in only 1 G1b-infected patient, in association with L159F and C316N (see Fig. 4A).

In summary, although these patients had all failed the same DAA regimen, each HCV subtype showed a different pattern of RAS (Fig. 4A).

3.4.2. Simeprevir [SMV] + Sofosbuvir [SOF] (n = 39)

NS3 substitutions at position 168 (D168 A/E/V/T/Y) were the most prevalent RAS in G1a, G1b, and G4d. Q80R/K were found in G1b and G4d, while R155K appeared only in G1a and R155Q only in G1b. As to the NS5B region, 16/28 (57.1%) and 18/28 (64.3%) patients carried L159F and C316N, respectively, at the time of the analysis (Fig. 4B).

3.4.3. Daclatasvir [DCV] + Sofosbuvir [SOF] (n = 35)

RAS resistance to DCV was characterized by the Y93H mutation in G1a, G1b, and G3a, followed by L31I/M/V and at positions 30 and 28 (Fig. 4C). The NS5B RAS, L159F and C316N, appeared exclusively in G1b (3/6, 50% of patients).

Interestingly, all G1b patients with L159F + C316N in NS5B had L31I/M/V + Y93H in NS5A. Moreover, in two of the three G1b patients carrying the L159F + C316N + L31I/V + Y93H four-mutant combination in the same genome, S282T, a well-recognized SOF resistance mutation, was also present (Fig. 4C).

In G3a patients, the A30K substitution never appeared in combination with Y93H, which could suggest a restriction for co-selection of these RAS in the same genome. There was a notable absence of RAS in NS5B except in 1 patient who carried the high-resistance S282T alone in 100% of the viral genomes sequenced (Fig. 4C).
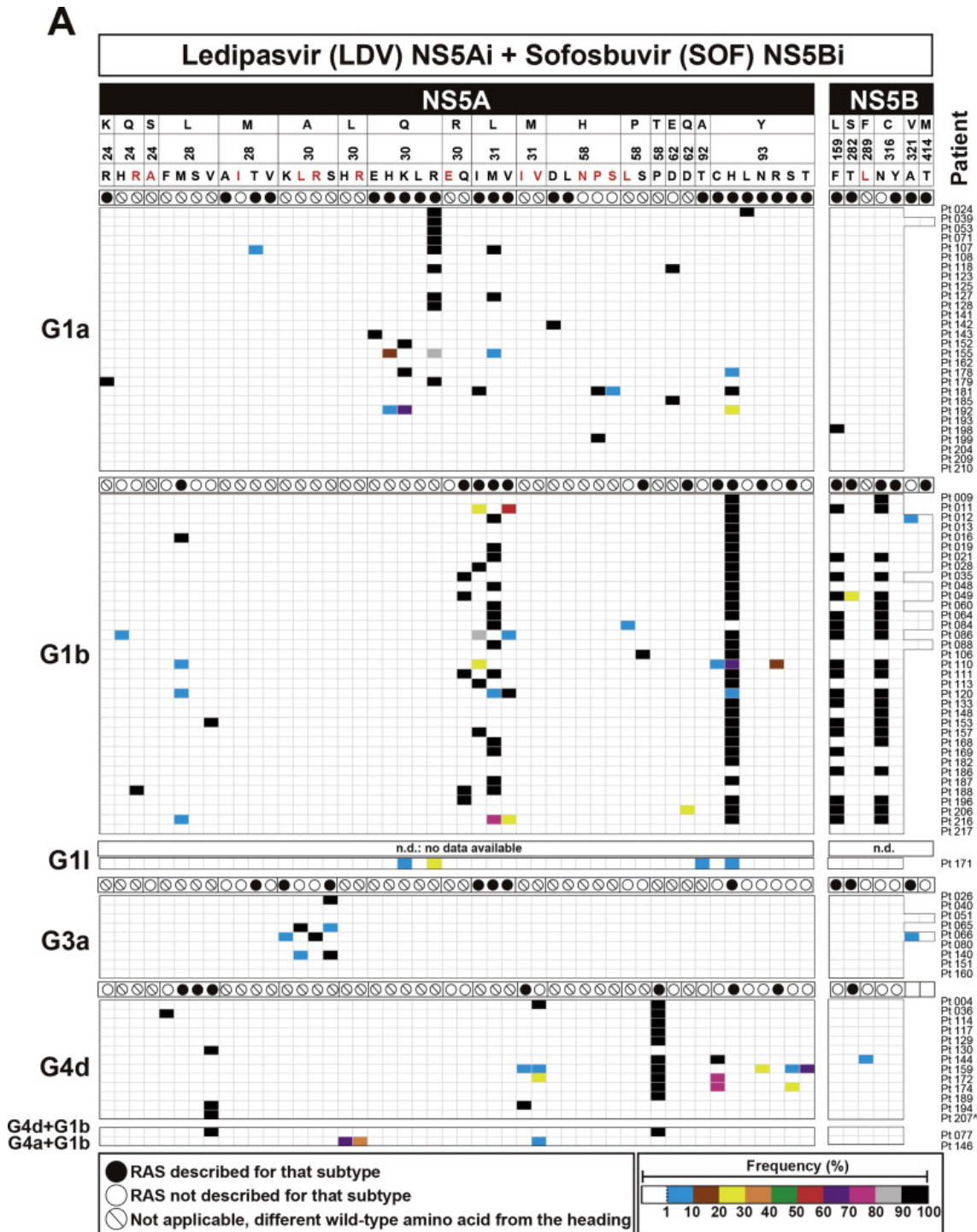
3.4.4. Paritaprevir/ritonavir [PRV/r] + Ombitasvir [OMV] + Dasabuvir [DSV] (n = 20)

No dominant RAS were observed in NS3, but most of those found were at positions 56, 80, and 168 (Fig. 4D). In NS5A, the dominant RAS in G1a patients were at positions 30 and 28, whereas the most prevalent RAS in G1b were Y93H and R30Q.

Resistance to the allosteric NS5B inhibitor DSV included L159F, C316N, V321A, and S556G in G1b, and C316Y, M414T, and A421V in G1a.

3.4.5. SOF-treated patients (n = 174)

In all SOF-based combinations, RAS in NS5B were almost exclusively found in G1b-infected patients (Figs. 4A, B, 4C), and 32.2% (56/174) of patients in this group had RAS mutations in viral regions that were not targeted by the drug they received (extra-target).
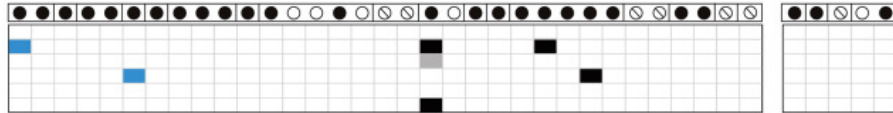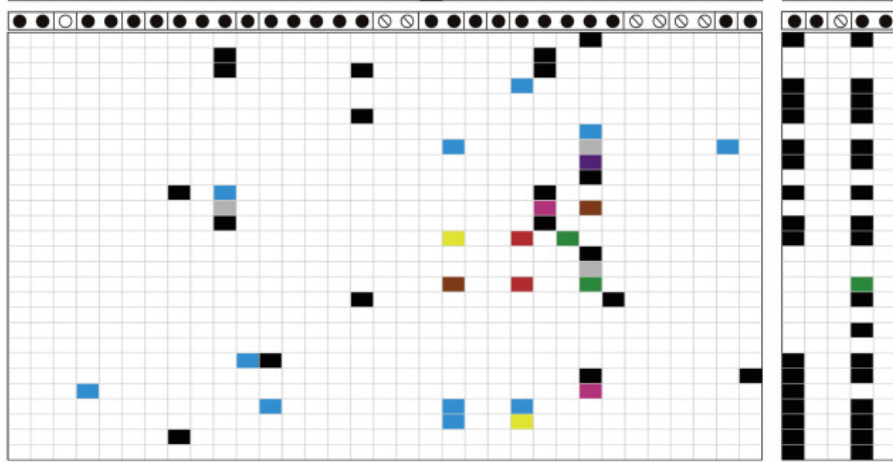
B

Simeprevir (SMV) NS3i + Sofosbuvir (SOF) NS5Bi

C

Daclatasvir (DCV) NS5Ai + Sofosbuvir (SOF) NS5Bi

D

Paritaprevir / ritonavir (PTV/r) NS3i + Ombitasvir (OMV) NS5Ai + Dasabuvir (DSV) NS5Bi

Fig. 4. Heat map of RAS divided according to DAA treatment (A to D). The HCV subtype is given on the left, the treatment in the upper empty boxes and the target protein in the upper filled boxes, above the amino acid replacements. Amino acids depicted in red indicate changes previously described as RAS, but with a different wild-type (parental) amino acid than the one indicated. Under each RAS, black-filled circles mean that the RAS has been previously described for that subtype, empty circles indicate that the RAS was not previously described for that subtype, and crossed circles identify RAS that have been reported, but with a different wild-type amino acid at that position. A) Ledipasvir + sofosbuvir (N = 88) with a mean sampling time after EOT of 21 weeks (data available for 56/88 patients); B) Simeprevir + sofosbuvir (N = 39); with a mean sampling time after EOT of 31 weeks (data available for 23/39 patients); C) Daclatasvir + sofosbuvir (N = 35) with a mean sampling time after EOT of 30 weeks (data available for 18/35 patients); D) Paritaprevir/r + ombitasvir + dasabuvir (N = 20) with a mean sampling time after EOT of 33 weeks (data available for 12/20 patients). The color code for RAS frequency is that same as in Fig. 2.

^Patient who has failed two different treatments.
*Patient who has failed two different treatments.

3.5. RAS quantity profile at failure

An overview of the RAS detected by subtype and failed treatment shows that a larger number of RAS were seen at failure in G1a and G1b-infected patients than in those with other subtypes, regardless of the treatment received (Fig. 5 and S2). In addition, the RAS response pattern to triple therapy (3D) differed from the response to SOF-based treatments in some genotypes. There were no NS5B mutations in G3a patients receiving 3D, but this region was affected in G3a patients receiving SOF. No such differences were found in G1a and G1b patients. (Fig. S2).

3.6. RAS combination profiles

Several RAS combinations were observed in G1b-infected patients who failed LDV/DCV + SOF (Fig. 6). In the NS5A region, L31I/M/V was combined with Y93H in a high percentage of patients, and especially after ledipasvir-based treatment. These RAS confer a high level of resistance to DAAs in subtypes G1a and G1b. Specifically, L31M + Y93H confer increased resistance to daclatasvir, with a 4200 to 16,000-fold change (FC) in G1b patients, and to elbasvir (FC = 7568 for G1a and 5000 for G1b), ledipasvir (FC = 20,270 for G1b), ombitasvir (FC = 142-12,323 for G1b), pibrentasvir (FC = 195 for G1a and 0.7 for G1b), and velpatasvir (FC = 44 for G1b). The L31V + Y93H combination confers resistance to daclatasvir (FC = 166,667 for G1a and 8336-4789 for G1b), elbasvir (FC = 53571 for G1a), and ombitasvir (FC = 12,328 for G1b) (Sorbo et al., 2018).

In the NS5B region, L159F + C316N were combined in the same genome in almost half of G1b-infected patients, and quadruple RAS combinations in NS5A + NS5B emerged in 16.7% of patients after LDV/DCV + SOF treatment (Fig. 6).

In SMV + SOF-treated patients, the Q80R + D168E combination in NS3, which confers a 418-fold increase in SMV resistance in vitro (Lontok et al., 2015), was associated with L159F + C316N in NS5B in 2/28 (7.1%) G1b-infected patients. D168V, which confers a 3100-fold increase in resistance to SMV in vitro, was associated with L159F + C316N in 4/28 (14.3%) G1b patients.

3D therapy was especially prone to emergence of multiple RAS combinations, including a quintuple combination in 2/7 (28.6%) G1b-infected patients (Fig. 6).

On analysis of haplotype frequencies, the L31M + Y93H combination appeared at frequencies >90% in 12/16 (75%) G1b-infected patients who failed LDV/DCV + SOF, whereas L31I + Y93H and L31V + Y93H showed a wider range of frequencies (Table S3.1 and S3.2). In G1b SMV + SOF failures, the Q80R + D168E combination was detected at frequencies >80% in all except 1 case. On the other hand, the R155Q + D168A combination appeared at frequencies of <20% in all patients (Table S3.3). Moreover, after 3D treatment, Y56H + D168V and R30Q + Y93H were both found in 5/6 (83.3%) patients (Table S3.4). The NS5B L159F + C316N combination prevailed at frequencies >98% in all viral isolates where it had been observed, regardless of the failed regimen (Table S3.2, S3.3, and 3.4).
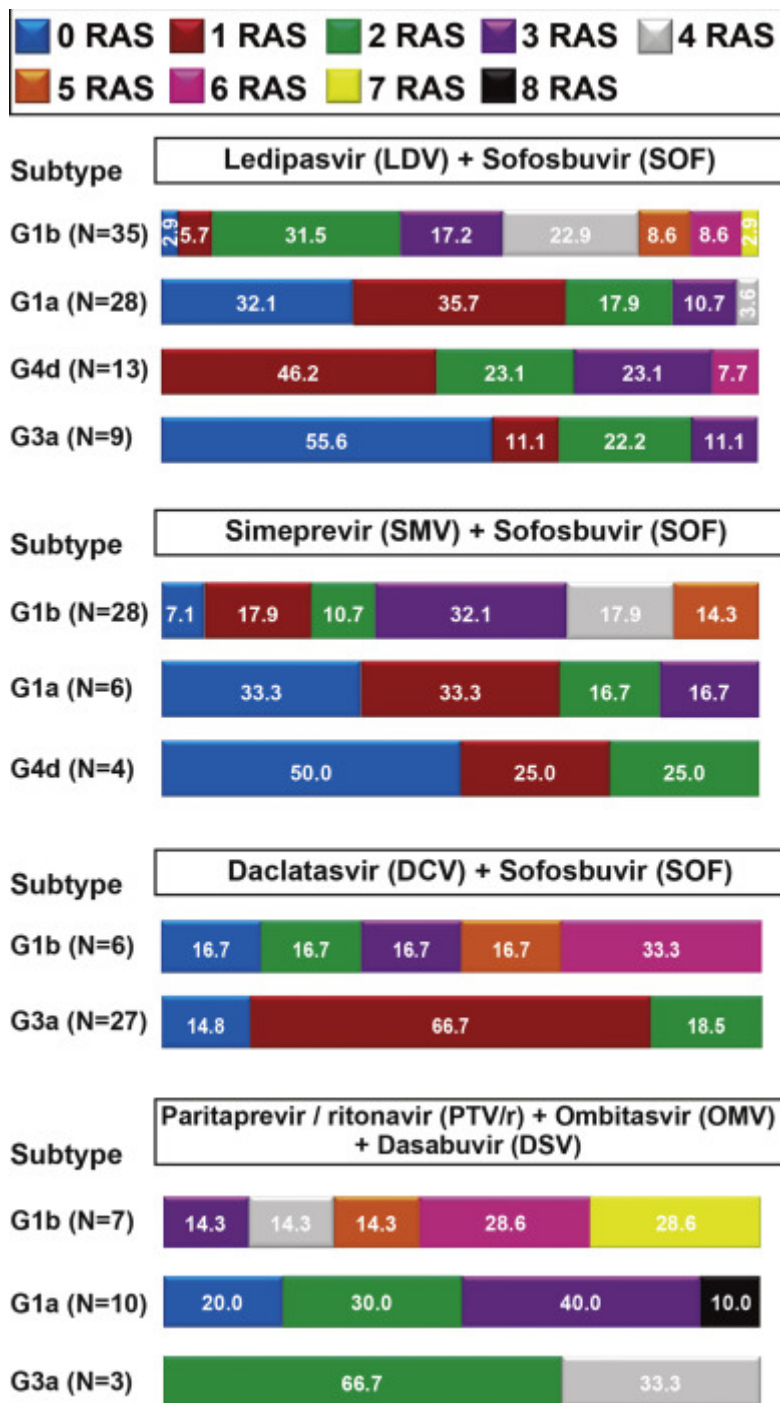
Fig. 5. RAS quantity profile according to subtypes and treatment failure (empty boxes). HCV subtype and number of patients are given on the left. The percentage of patients carrying different total numbers of RAS at treatment failure are indicated by the number and color code within the boxes on the right.
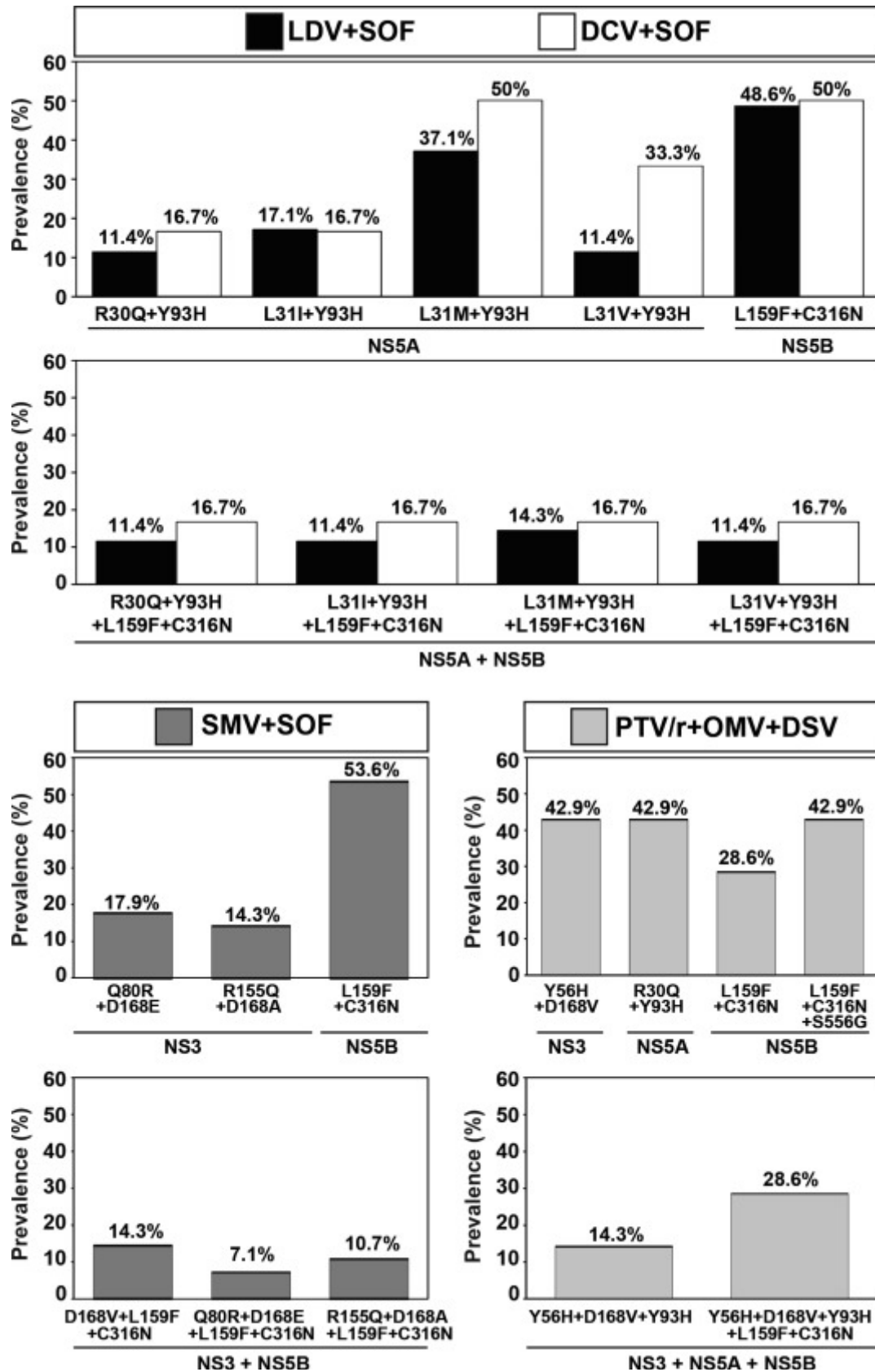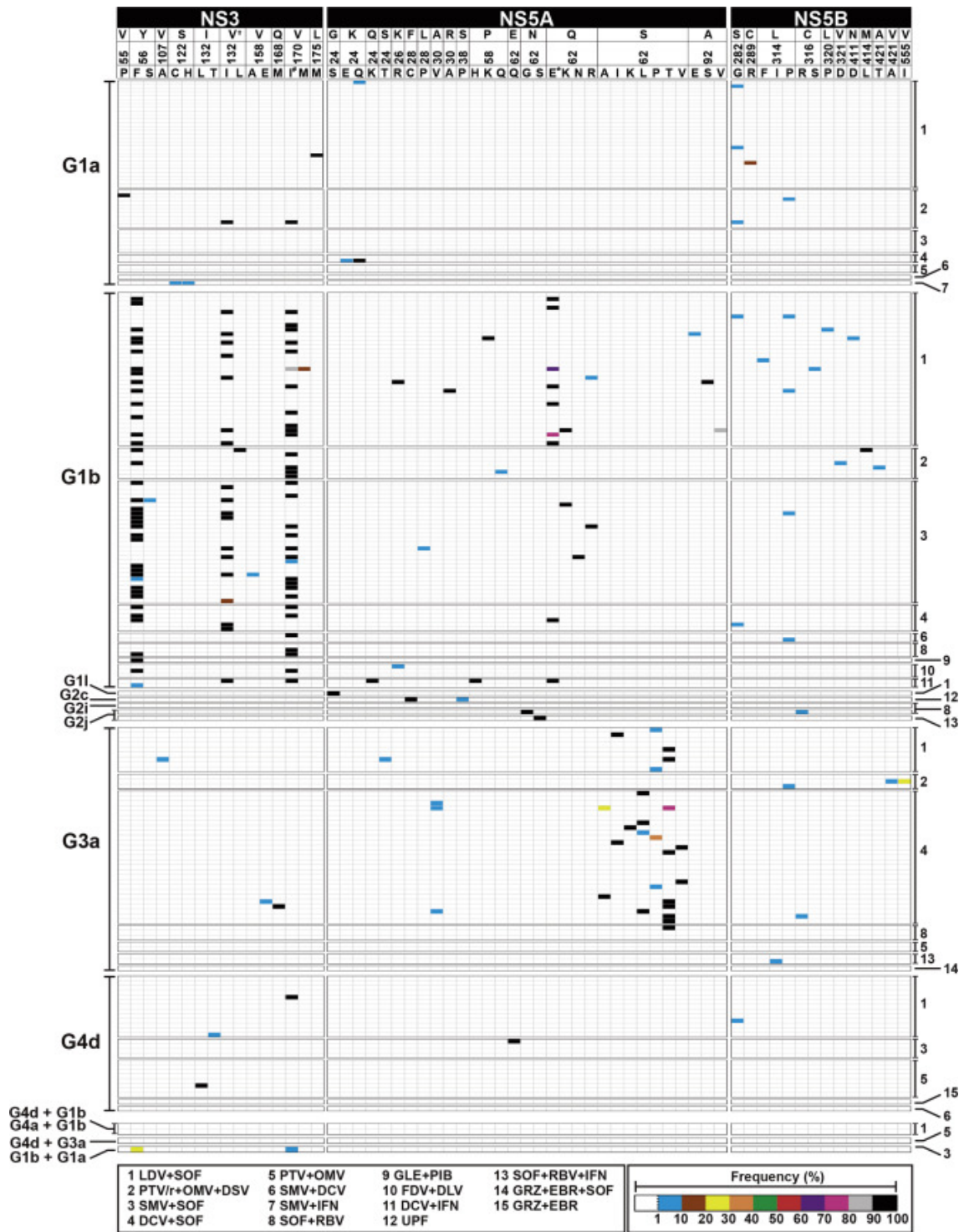
Fig. 6. Percentage of G1b patients carrying resistance-associated substitution (RAS) combinations at single and multiple target regions. In overlapped combination profiles, patients carrying each combination are mutually excluded. LDV+SOF (n=36); DCV+SOF (N=6); SMV+SOF (N=28); PTV/r+OMV+DSV (N=7).

Fig. 7. Heat map of putative new RAS. Schematic representation of the prevalence of amino acid changes detected in our cohort study, but not described as bona fide RAS in the literature. Display and symbols are the same as in Figures 2 and 4. Symbols in amino acids (upper part of the figure) include (Ɨ) in V132, which means that I132V was a RAS described for G1a, and (#) in I170, which indicates that both V and I are wild-type amino acids described for G1a and G1b.

3.7. Putative new resistance-associated substitutions

An overview of the amino acid sequence patterns in NS3, NS5A, and NS5B (Fig. 2, Fig. 4) distinguished 3 possible outcomes following treatment failure: 1) no RAS detected in any region analyzed, 2) presence of well-known RAS (Fig. 2), and 3) previously undescribed amino acid substitutions found in a residue corresponding to a known RAS (Fig. 7). The new substitutions at previously assigned RAS positions included Y56F, V132I, and V170I in NS3 for G1b, A30V in NS5A for G3a, and S282G in NS5B for G1a and G1b. For example, Y56F was found in most GT1b patients at failure. In addition, variants at position 62 in NS5A were also repeatedly observed in G1b- and G3a-infected patients, regardless of the treatment received. L314P in NS5B was the only RAS found in G1a, G1b, and G3a.

4. Discussion

In a large cohort of HCV-infected patients who failed DAA therapy, emergent RAS were classified by viral subtype, target protein, and antiviral treatment. There was evidence of a considerable influence of viral subtype on the development of specific mutations. These results were obtained using NGS in a clinical diagnostic laboratory that provides support to the publicly-funded Spanish healthcare system. The method can generate a report describing the number and frequency of minor and major RAS in the viral sample, and whether two or more mutations are combined in the same genome. Hence, the NGS protocol developed may be a good candidate to serve as a standardized test for HCV RAS detection to guide retreatment decisions when needed (EASL, 2018).

The 220 samples included underwent high-resolution HCV subtyping before RAS analysis so that subtype-specific primers could be used with deep sequencing. Surprisingly, of the 100 samples genotyped at the hospital of origin, 7 (7%) had been assigned a different genotype than that determined in the high-resolution analysis. Hence, it is possible that these patients had received suboptimal treatments according to their genotype (EASL, 2018), which may have facilitated RAS selection and DAA treatment failure (Dietz et al., 2018; EASL, 2018; Sarrazin, 2016; AASLD, 2017; Di Maio et al., 2017; Pawlotsky, 2016; Zeuzem et al., 2017). In a study investigating the consequences of inaccurate genotyping, Polilli et al. cited potential prescription of suboptimal therapy and remarkable increases in treatment costs (Polilli et al., 2016).

In our study, the number and type of RAS detected did not differ significantly between treatments including or not ribavirin. This finding may support addition of ribavirin to retreatment regimens, as the potential mutagenic effect of the drug did not significantly change RAS frequencies.

We found that 88.6% of patients carried one or more RAS. Poor response rates to retreatment with the same DAA regimen (Lawitz et al., 2015) suggest that switching DAA class is indicated in salvage treatments. However, the presence of various RAS in the same viral genome causing a dramatic increase in resistance to the inhibitor and cross-resistance to inhibitors of the same type, together with the presence of extra-target RAS (Fig. 6, Fig. 7), may hamper this option (Sorbo et al., 2018). Blind treatment of resistant viruses using a pangenotypic triple combination is a possibility, but it carries the risk of multiresistant virus selection. In these patients, NGS resistance testing could be useful to guide treatment decisions and to document RAS elimination on follow-up (Sarrazin, 2016; Krishnan et al., 2015; Susser et al., 2011; Thomas et al., 2011; Buti et al., 2016; Svarovskaia et al., 2014; Dvory-Sobol et al., 2015). The absence of RAS should be ascertained by NGS because the viral quasispecies "memory" from previous treatments may favor selection of HCV escape mutants, as has been reported in human immunodeficiency virus (HIV) patients (Briones et al., 2006).

The basic features of RNA viral genetics can explain the diversity of RAS and their wide range of frequencies in these infections. First, bona fide RAS can increase in frequency depending on the fitness cost they inflict. In addition, substitutions can occur in genomes on their way to dominance and be hitchhiked towards various frequency levels. Some substitutions may play strong or minor compensatory roles on the bona fide RAS substitutions. Furthermore, RNA viruses can find multiple mutational pathways (ie, alternative RAS) in response to selective constraints, thereby increasing their replicative fitness (Gallego et al., 2018).

In contrast to the situation before first-line therapy, the viral population emerging at completion of treatment has a history of replication in the presence of antiviral agents. These RAS may have a greater impact on resistance than the same RAS detected at baseline, as viral adaptation to growth in the presence of drugs may have co-selected compensatory mutations (EASL, 2018; Domingo et al., 2001; Domingo, 2016). For example, in G1b-infected patients receiving DSV-based treatments, L159F and C316N emergence in the NS5B palm 2 domain (Donaldson et al., 2015), a site distant from the palm 1 domain where most DSV RAS have been mapped (Kati et al., 2015), suggests that extra-target mutations at palm 2 may act as compensatory structural changes. Thus, L159F + C316N might jeopardize salvage treatment with other NS5B inhibitors (Hang et al., 2009).

Our results show that the RAS profile is to some degree subtype-dependent and that it can differ even in the presence of 2 different antiviral agents of the same class (eg, the NS5A inhibitors LDV and DCV). Furthermore, certain high-frequency RAS, such as Q30R in NS5A for G1a, Y93H in NS5A for G1b and G3a, and L159F and C316N in NS5B for G1b, emerged regardless of the drugs administered. As to the number of RAS and their combinations, G1b-infected patients showed the most variable profile, followed by G1a, G4d, and G3a, with all treatments. This suggests that G1b may require a larger number of RAS than other subtypes to achieve comparable resistance levels.

A considerable percentage of G1a-, G3a-, and G4d-infected patients showed no known RAS, despite treatment failure. Viral escape in the absence of RAS can be associated with unconfessed poor adherence to treatment, a deficient host immune response, or inappropriate timing of virus isolation for RAS analysis (Buti et al., 2016). The clinical reports made poor adherence or a deficient immune response unlikely in most of the patients studied. Hence, this point should be investigated in view of similar observations in other patient cohorts (Dietz et al., 2018; Di Maio et al., 2017), and previous evidence in cell culture that HCV fitness may be a determinant of RAS-independent resistance (Gallego et al., 2016; Sheldon et al., 2014).

As an additional complication to RAS analysis, amino acids that confer a RAS phenotype in one subtype may be present in wild-type sequences of another subtype. Moreover, several new substitutions, such as Y56F in NS3, are being accepted as RAS (EASL, 2018; Sorbo et al., 2018). Although these mutations are not yet validated as bona fide RAS, they should be considered when designing salvage treatments, and in vitro studies should be done to investigate their contribution to resistance.

Most studies on HCV RAS have used Sanger sequencing, and have suggested that this method would suffice to detect most clinically significant RAS (Sarrazin et al., 2016), even though mutants present at frequencies below 15%–25% would be excluded (Quinones-Mateu et al., 2014). In our cohort, around 19% of patients had RAS frequencies in the range of 1%–20%, and some of them carried RAS combinations in the same genome. Low-frequency RAS have also been reported in other cohorts (Kai et al., 2017), and one study has shown that RAS present at frequencies of less than 15% can be selected as majority variants following treatment (Perales et al., 2018). NGS enables quantification of genomes carrying a combination of different RAS per amplicon with high confidence when more than 10,000 reads per amplicon are obtained, with a 1% cut-off value (Gregori et al., 2013), enabling detection of these minority variants.

Additional experience with NGS will define the practical value of deep-sequencing RAS detection in DAA failures. Fortunately, triple therapy with voxilaprevir + velpatasvir + sofosbuvir is a highly effective retreatment regimen in most cases, including patients with RAS. Nonetheless, caution must be exercised when treating patients with viral resistance mutations in 2 protein targets because of the risk of selecting genomes resistant to the 3 inhibitors and inducing cross resistance to other inhibitors of the same drug class. This could be a special concern for specific subtypes and after failure to NS5Ai + NS5Bi double therapies. It is reasonable to think that in clinical practice, some treatment failures will be a challenge for retreatment and require RAS-tailored rescue therapy. Complex patients with comorbidities requiring medication that can reduce the efficacy of DAAs by drug-drug interactions could also benefit from individualized therapy. For example, those receiving strong anti-epileptic drugs (AEDs) such as carbamazepine, phenytoin and phenobarbital (van Seyen et al., 2019), which activate CYP 3A4 and thereby, lower the effective dose of several HCV inhibitors.

5. Conclusions

In summary, NGS analysis in a cohort of HCV-infected patients failing DAA treatment documented a complex array of amino acid substitutions in treatment-targeted proteins. The analysis showed subtype-specific substitutions and multiple alternative minority sequences in viruses that survived treatment. These findings in real-life clinical samples indicate that HCV drug resistance testing based on deep-sequencing before retreatment could be useful for designing salvage therapies, particularly in difficult-to-treat cases. The increasing descriptions of naturally occurring RAS in treatment-naïve patients, as well as RAS in extra-target regions, begs for further studies to understand their clinical meaning in relation to DAA therapy, and NGS RAS testing could also be useful in this scenario. Finally, RAS listing may be a valuable component in the worldwide effort to eliminate HCV infection as a public health threat, as advocated by the World Health Organization.

Declaration of competing interest

We declare that no public or private company has had any role in the study design, data collection, experimental work, data analysis, decision to publish, or preparation of the manuscript. Roche Diagnostics S.L. provided support in the form of a salary for one of the authors [Josep Gregori], but the company did not have any additional role in the study design, data collection and analysis, decision to publish, or preparation of the manuscript.

No other Competing Interests to declare. Thus, our adherence to Antiviral Research policies on sharing data and materials is not altered.

Abbreviations

HCV	hepatitis C virus
RAS	resistance-associated substitutions
DAA	direct-acting antiviral
SVR	sustained virological response
NS3i	nonstructural region 3 inhibitor
PTV	paritapevir
r	ritonavir
SMV	simeprevir
GLE	glecaprevir
FDV	faldaprevir
GZR	grazoprevir
NS5Ai	NS5A inhibitor

DCV   daclatasvir
LDV   ledipasvir
OMV   ombitasvir
EBR   elbasvir
PIB   pibrentasvir
NS5Bi   N5B inhibitor
SOF   sofosbuvir
DSV   dasabuvir
DLV   deleobuvir
UPF   uprifosbuvir
RBV   ribavirin
IFN-α   interferon-α
EOT   end-of-treatment
HRCS   high-resolution HCV subtyping
G1a   genotype 1 subtype a
Y93H   Y wild type amino acid residue; 93 relates to position; H is the mutated genome

References

AASLD HCV guidance: recommendations for testing, managing, and treating hepatitis C. https://www.hcvguidelines.org/. 2017 Sep 21.

Briones, C., de, V.A., Molina-Paris, C., Domingo, E., 2006 Dec 15. Minority memory genomes can influence the evolution of HIV-1 quasispecies in vivo. Gene 384, 129–138.

Buti, M., Riveiro-Barciela, M., Esteban, R., 2015 Dec. Management of direct-acting antiviral agent failures. J. Hepatol. 63 (6), 1511–1522.

Buti, M., Gordon, S.C., Zuckerman, E., Lawitz, E., Calleja, J.L., Hofer, H., et al., 2016 Jan 1. Grazoprevir, elbasvir, and ribavirin for chronic hepatitis C virus genotype 1 infection after failure of pegylated interferon and ribavirin with an earlier-generation protease inhibitor: final 24-week results from C-salvage. Clin. Infect. Dis. 62 (1), 32–36.

Di Maio, V., Cento, V., Lenci, I., Aragri, M., Rossi, P., Barbaliscia, S., et al., 2017 Apr. Multiclass HCV resistance to direct-acting antiviral failure in real-life patients advocates for tailored second-line therapies. Liver Int. 37 (4), 514–528.

Dietz, J., Susser, S., Vermehren, J., Peiffer, K.H., Grammatikos, G., Berger, A., et al., 2018 Mar. Patterns of resistance-associated substitutions in patients with chronic HCV infection following treatment with direct-acting antivirals. Gastroenterology 154 (4), 976–988.

Domingo, E., 2016. Virus as Populations. Composition, Complexity, Dynamics and Biological Implications. Virus as Populations, first ed. ed. Academic Press, Elsevier, London, pp. 1–412.

Domingo, E., Biebricher, C.K., Eigen, M., Holland, J.J., 2001. Quasispecies and RNA virus evolution. In: Landes Biosciences. Georgetown, Texas. USA.

Donaldson, E.F., Harrington, P.R., O'Rear, J.J., Naeger, L.K., 2015 Jan. Clinical evidence and bioinformatics characterization of potential hepatitis C virus resistance pathways for sofosbuvir. Hepatology 61 (1), 56–65.

Dvory-Sobol, H., Wyles, D., Ouyang, W., Chodavarapu, K., McNally, J., Cheng, W., et al., 2015. Long-term persistence of HCV NS5A variants after treatment with NS5A inhibitor ledipasvir. J. Hepatol. 62, S221.

EASL, 2018 Aug. EASL recommendations on treatment of hepatitis C 2018. J. Hepatol. 69 (2), 61–511.

Gallego, I., Sheldon, J., Moreno, E., Gregori, J., Quer, J., Esteban, J., et al., 2016. Barrierindependent, fitness-associated differences in sofosbuvir-efficacy against hepatitis C virus. Antimicrob. Agents Chemother. 60 (6), 3786–3793.

Gallego, I., Gregori, J., Soria, M.E., Garcia-Crespo, C., Garcia-Alvarez, M., Gomez-Gonzalez, A., et al., 2018 Oct. Resistance of high fitness hepatitis C virus to lethal mutagenesis. Virology 523, 100–109.

Gregori, J., Esteban, J.I., Cubero, M., Garcia-Cehic, D., Perales, C., Casillas, R., et al., 2013. Ultra-deep pyrosequencing (UDPS) data treatment to study amplicon HCV minor variants. PLoS One 8 (12), e83361.

Hang, J.Q., Yang, Y., Harris, S.F., Leveque, V., Whittington, H.J., Rajyaguru, S., et al., 2009 Jun 5. Slow binding inhibition and mechanism of resistance of non-nucleoside polymerase inhibitors of hepatitis C virus. J. Biol. Chem. 284 (23), 15517–15529.

Kai, Y., Hikita, H., Morishita, N., Murai, K., Nakabori, T., Iio, S., et al., 2017 Jan 30. Baseline quasispecies selection and novel mutations contribute to emerging resistance-associated substitutions in hepatitis C virus after direct-acting antiviral treatment. Sci. Rep. 7, 41660.

Kanda, T., Nirei, K., Matsumoto, N., Higuchi, T., Nakamura, H., Yamagami, H., et al., 2017 Dec 14. Retreatment of patients with treatment failure of direct-acting antivirals: focus on hepatitis C virus genotype 1b. World J. Gastroenterol. 23 (46), 8120–8127.

Kati, W., Koev, G., Irvin, M., Beyer, J., Liu, Y., Krishnan, P., et al., 2015 Mar. In vitro activity and resistance profile of dasabuvir, a nonnucleoside hepatitis C virus polymerase inhibitor. Antimicrob. Agents Chemother. 59 (3), 1505–1511.

Krishnan, P., Tripathi, R., Schnell, G., Reisch, T., Beyer, J., Dekhtyar, T., et al., 2015. Long-term follow-up of treatment-emergent resistance-associated variants in NS3, NS5A and NS5B with paritaprevir/r, ombitaavir- and dasabuvir-based regimens. J. Hepatol. 62, S220.

Lawitz, E., Flamm, S., Yang, J.C., Pang, P.S., Zhu, Y., Svarovskaia, E., et al., 2015. Retreatment of patients who failed 8 or 12 weeks of Ledipasvir/Sofosbuvir-based regimens with Ledipasvir/Sofosbuvir for 24 weeks. J. Hepatol. 62 (Suppl. 2), S192.

Lontok, E., Harrington, P., Howe, A., Kieffer, T., Lennerstrand, J., Lenz, O., et al., 2015 Nov. Hepatitis C virus drug resistance-associated substitutions: state of the art summary. Hepatology 62 (5), 1623–1632.

Ministry of health social services and equality, 2018. Strategic plan for tackling hepatitis C in the national health system. https://www.msssi.gob/ciudadanos/enfLesiones/enfTransmisibles/hepatitisC/PlanEstrategicoHEPATITITSC/docs/Plan Estrategico Abordaje Hepatitits C (PEAHC).pdf.

Ministry of health social services and equality, 2019. Strategic plan for tackling hepatitis C in the national health system. https://www.mscbs.gob.es/gabinete/notasPrensa. do?id=4353.

Pawlotsky, J.M., 2016 Jul. Hepatitis C virus resistance to direct-acting antiviral drugs in interferon-free regimens. Gastroenterology 151 (1), 70–86.

Perales, C., Chen, Q., Soria, M.E., Gregori, J., Garcia-Cehic, D., Nieto-Aponte, L., et al., 2018. Baseline hepatitis C virus resistance-associated substitutions present at frequencies lower than 15% may be clinically significant. Infect. Drug Resist. 11, 2207–2210.

Polaris Observatory HCV Collaborators, 2017 Mar. Global prevalence and genotype distribution of hepatitis C virus infection in 2015: a modelling study. Lancet Gastroenterol. Hepatol. 2 (3), 161–176.

Polilli, E., Cento, V., Restelli, U., Ceccherini-Silberstein, F., Aragri, M., Di, M.V., et al., 2016. Consequences of inaccurate hepatitis C virus genotyping on the costs of prescription of direct antiviral agents in an Italian district. Clinicoecon OuClinicoecon. Outcomes Res.tcomes Res 8, 467–473.

QSutils, 2018. Quasispecies Diversity. R Package Version 1.0.0. [computer program]. https://bioconductor.org/packages/release/bioc/html/QSutils.html.

Quer, J., Gregori, J., Rodriguez-Frias, F., Buti, M., Madejon, A., Perez-Del-Pulgar, S., et al., 2015 Jan. High-resolution hepatitis C virus subtyping using NS5B deep sequencing and phylogeny, an alternative to current methods. J. Clin. Microbiol. 53 (1), 219–226.

Quinones-Mateu, M.E., Avila, S., Reyes-Teran, G., Martinez, M.A., 2014 Sep. Deep sequencing: becoming a critical tool in clinical virology. J. Clin. Virol. 61 (1), 9–19.

Rodriguez-Frias, F., Nieto-Aponte, L., Gregori, J., Garcia-Cehic, D., Casillas, R., Tabernero, D., et al., 2017 Oct. High HCV subtype heterogeneity in a chronically infected general population revealed by high-resolution hepatitis C virus subtyping. Clin. Microbiol. Infect. 23 (10), 775e1–775e6.

Sarrazin, C., 2016. The importance of resistance to direct antiviral drugs in HCV infection in clinical practice. J. Hepatol. 64, 486–504.

Sarrazin, C., Dvory-Sobol, H., Svarovskaia, E.S., Doehle, B.P., Pang, P.S., Chuang, S.M., et al., 2016 Sep. Prevalence of resistance-associated substitutions in HCV NS5A, NS5B, or NS3 and outcomes of treatment with ledipasvir and sofosbuvir. Gastroenterology 151 (3), 501–512.

Sheldon, J., Beach, N.M., Moreno, E., Gallego, I., Pineiro, D., Martinez-Salas, E., et al., 2014 Oct. Increased replicative fitness can lead to decreased drug sensitivity of hepatitis C virus. J. Virol. 88 (20), 12098–12111.

Sorbo, M.C., Cento, V., Di M, V., Howe, A.Y.M., Garcia, F., Perno, C.F., et al., 2018 Mar. Hepatitis C virus drug resistance associated substitutions and their clinical relevance: update 2018. Drug Resist. Updates 37, 17–39.

Soria, M.E., Gregori, J., Chen, Q., Garcia-Cehic, D., Llorens, M., de Avila, A.I., et al., 2018 Sep 3. Pipeline for specific subtype amplification and drug resistance detection in hepatitis C virus. MC Infect. Dis. 18 (1), 446. https://doi.org/10.1186/s12879-018-3356-6.

Susser, S., Vermehren, J., Forestier, N., Welker, M.W., Grigorian, N., Fuller, C., et al., 2011 Dec. Analysis of long-term persistence of resistance mutations within the hepatitis C virus NS3 protease after treatment with telaprevir or boceprevir. J. Clin. Virol. 52 (4), 321–327.

Svarovskaia, E.S., Dvory-Sobol, H., Parkin, N., Hebner, C., Gontcharova, V., Martin, R., et al., 2014 Dec 15. Infrequent development of resistance in genotype 1-6 hepatitis C virus-infected subjects treated with sofosbuvir in phase 2 and 3 clinical trials. Clin. Infect. Dis. 59 (12), 1666–1674.

Thomas, X.V., de Bruijne, J., Kieffer, T.L., Sullivan, J.C., Rebers, S., de Vries, M., et al., 2011. Long-term follow-up of chronic hepatitis C infected patients treated with telaprevir: evaluation of persistence of resistant variants by ultra-deep sequencing. J. Hepatol. 54 (Suppl. 1), S490–S491.

United Nations-General Assembly, 2017. Global hepatitis report. WHO; 2017 Apr 21. Report No.: 2017/pp.1–83. http://www.who.int/hepatitis/publications/globalhepatitis-report2017/en/.

van Seyen, M., Smolders, E.J., van Wijngaarden, P., Drenth, J.P.H., Wouthuyzen-Bakker, M., de Knegt, R.J., et al., 2019 Mar. Successful HCV treatment of patients on contraindicated anti-epileptic drugs: role of drug level monitoring. J. Hepatol. 70 (3), 552–554.

Vermehren, J., Sarrazin, C., 2012 Aug. The role of resistance in HCV treatment. Best Pract. Res. Clin. Gastroenterol. 26 (4), 487–503.

Vermehren, J., Susser, S., Dietz, J., von Hahn, T., Petersen, J., Hinrichsen, H., et al., 2016. Retreatment of patients who failed DAA-combination therapies:real-world experience from a large hepatitis C resistance database. J. Hepatol. 64 (2), S188.

Zeuzem, S., Mizokami, M., Pianko, S., Mangia, A., Han, K.H., Martin, R., et al., 2017 May. NS5A resistance-associated substitutions in patients with genotype 1 hepatitis C virus: prevalence and effect on treatment outcome. J. Hepatol. 66 (5), 910–918.